Promega

Spectrum Compact CE System

Sanger Sequencing and Fragment/STR Analysis

- benchtop 4-capillary electrophoresis instrument for 4-, 5- and 6-dye chemistries and up to 32 samples in a single run
- compatible with a broad range of commercial chemistries for DNA sequencing, forensic STR profiling, MLPA, MSI and many more
- flexible raw data analysis
- prefilled, plug-and-play consumables for maximal flexibility and efficiency
- controlled by the integrated touchscreen or by Remote Access Software
- on-site instrument and software installation, operational and application trainings

www.promega.com/spectrum-compact-system

Spectrum
COMPACT
CE SYSTEM

Received: 23 October 2018 | Revised: 17 April 2019 | Accepted: 24 April 2019

DOI: 10.1002/humu.23775

BRIEF REPORT

WILEY Human Mutation HGVS HUMAN GENOME VARIATION SOCIETY

Multigenic truncation of the semaphorin–plexin pathway by a germline chromothriptic rearrangement associated with Moebius syndrome

Lusine Nazaryan-Petersen[1] | Inês R. Oliveira[1,2] | Mana M. Mehrjouy[1] | Juan M. M. Mendez[1] | Mads Bak[1,3] | Merete Bugge[1] | Vera M. Kalscheuer[4] | Iben Bache[1,3] | Dustin C. Hancks[5] | Niels Tommerup[1]

[1]Wilhelm Johannsen Center for Functional Genome Research, Department of Cellular and Molecular Medicine, University of Copenhagen, Copenhagen, Denmark

[2]Department of Regulation and Evaluation of Medicines and Health products, Faculty of Pharmacy, University of Lisbon, Lisbon, Portugal

[3]Department of Clinical Genetics, Rigshospitalet, Copenhagen University Hospital, Copenhagen, Denmark

[4]Research Group Development and Disease, Max Planck Institute for Molecular Genetics, Berlin, Germany

[5]Department of Immunology, The University of Texas Southwestern Medical Center, Dallas, Texas

Correspondence
Lusine Nazaryan-Petersen and Niels Tommerup, Wilhelm Johannsen Center for Functional Genome Research, Institute of Cellular and Molecular Medicine, University of Copenhagen, Blegdamsvej 3B, 2200, Copenhagen N, Denmark.
Email: nlusine@sund.ku.dk (L. N. P.); ntommerup@sund.ku.dk (N. T.)

Funding information
NIH K99/R00 Pathway to Independence Award (NIGMS); Det Frie Forskningsråd, Grant/Award Number: 4183-00482B; Cancer Prevention Research Institute of Texas (CPRIT) Recruitment Award; Lundbeckfonden, Grant/Award Number: 2013–14290; University of Copenhagen Excellence Programme for Interdisciplinary Research (Global Genes, Local Concerns); Danish Council for Independent Research

Abstract

Moebius syndrome (MBS) is a congenital disorder caused by paralysis of the facial and abducens nerves. Although a number of candidate genes have been suspected, so far only mutations in *PLXND1* and *REV3L* are confirmed to cause MBS. Here, we fine mapped the breakpoints of a complex chromosomal rearrangement (CCR) 46,XY,t(7;8;11;13) in a patient with MBS, which revealed 41 clustered breakpoints with typical hallmarks of chromothripsis. Among 12 truncated protein-coding genes, SEMA3A is known to bind to the MBS-associated PLXND1. Intriguingly, the CCR also truncated *PIK3CG*, which in silico interacts with REVL3 encoded by the other known MBS-gene *REV3L*, and with the SEMA3A/PLXND1 complex via FLT1. Additional studies of other complex rearrangements may reveal whether the multiple breakpoints in germline chromothripsis may predispose to complex multigenic disorders.

KEYWORDS
chromothripsis, Moebius syndrome, *PIK3CG*, *SEMA3A*, *SEMA3D*

Moebius syndrome (MBS; MIM# 157900) is a congenital disorder with malformations of orofacial structures and the limbs, largely caused by unilateral or bilateral paralysis of the facial and abducens nerves (Kadakia, Helman, Schwedhelm, Saman, & Azizzadeh, 2015). MBS is characterized by patients' masklike facial expression caused by their inability to smile, frown, or raise an eyebrow, which may lead to emotional or social adjustment issues (Broussard & Borazjani, 2008).

The aetiology of MBS is not fully understood, however, genetic defects, abnormal vascular supply during embryogenesis and environmental toxic factors leading to abnormal brainstem development have been considered to be involved (D'Cruz, Swisher, Jaradeh, Tang, & Konkol, 1993; Kadakia et al., 2015; Verzijl, van der Zwaag, Cruysberg, & Padberg, 2003). A genetic aetiology for MBS was suggested by several familiar cases with MBS, where both autosomal dominant (Kremer et al., 1996; Ziter, Wiser, & Robinson, 1977) and recessive (Donahue, Wenger, Steele, & Gorin, 1993) modes of inheritance have been described. Linkage analysis and chromosomal abnormalities have provided evidence for specific loci at 1p22, 3q21–q22, 10q21.3–q22.1, and 13q12.2–13, where several candidate genes have been proposed due to functional relevance (Table S1; Kadakia et al., 2015). Sequencing studies have so far not identified mutations in specific genes at these loci (Uzumcu et al., 2009; van der Zwaag et al., 2002, 2004), but a recent study of 103 MBS patients revealed mutations in the genes *PLXND1* (MIM# 604282) and *REV3L* (MIM# 602776; Tomas-Roca et al., 2015). In addition, mutations in *TUBB3* (MIM# 602661) have been identified in two patients with overlapping MBS symptoms (Nakamura, Matsumoto, Zaha, Uematsu, & Nonoyama, 2018; Patel et al., 2017).

Here, using next-generation mate-pair sequencing, we provide detailed genomic mapping and characterization of the breakpoint junctions (BPJs) of a previously reported complex chromosomal rearrangement (CCR), 46,XY,t(7;8;11;13) (Borck et al., 2001). At that time, nine breakpoints were suggested: four located on 7q21.1-7q36; two on 8q21.3; two on 11p14.3, and one on 13q21.2. In the original chromosome analysis in 1976, no report of parental mosaicism was noted. Therefore, we concluded that this CCR is a de novo event. The patient had typical symptoms of MBS, such as micrognathia and congenital paresis of the facial muscles resulting in sucking and swallowing difficulties. In addition, gynecomastia was noted in the clinical description but it is unknown whether he had micropenis, delayed puberty, hypo/anosmia or other manifestations related to hypogonadotropic hypogonadism. He had severe intellectual disability with limited language. Hearing loss was noticed from the age of 50 years. He died at the age of 54 years. The patient's parents and two siblings were healthy. The study has been approved by the Danish Data Protection Agency (2012-54-0053) and written consent was obtained from the brother of the patient. Mate-pair libraries were prepared using Nextera mate-pair kit following the manufacturers' instructions (Illumina, San Diego, CA) and the final library was subjected to 2 × 100 base pair-end sequencing on an Illumina HiSeq. 2500 sequencing platform. FASTQ files were aligned to GRCh37 (hg19) using BWA-mem (http://arxiv:1303.3997v2). Only structural variations (SVs) with at least five confirming read-pairs were considered. Sample-specific SVs were identified by filtering the predicted SVs against DGV (Database of Genomic Variants; http://dgv.tcag.ca/dgv/app/home) and against an in-house database. The breakpoints (BPs) indicated by MPS analysis were further validated by polymerase chain reaction (PCR) and Sanger sequencing using standard procedures (primers and PCR conditions are provided in Table S3; Nazaryan et al., 2014). The BPJ sequences were split up at the breakpoint and aligned to genomic DNA of the breakpoint region to visualize indels, microhomology, insertions, and repeat elements within the breakpoint.

We used these molecular signatures at the BPJs to infer to the underlying mutational and repair mechanisms, for example, nonhomologous end-joining (NHEJ; Lieber, 2010); microhomology-mediated end-joining (MMEJ; McVey & Lee, 2008). The inserted L1M2 element at the BPJ 7-15_7-13 was checked for a possible underlying retrotransposition mechanism (Nazaryan-Petersen et al., 2016).

The identified truncated protein-coding genes and topological associated domains (TADs; Dixon et al., 2012; Rao et al., 2014) defined for human IMR90 fibroblasts (Table S2) at the breakpoints were analyzed for possible overlaps with known and candidate MBS genes (Table S1). The fused truncated genes with the same transcriptional orientation were evaluated in silico for the presence of open reading frames using the ExPASy Translate tool (http://www.expasy.org). We also performed in silico protein–protein interaction (PPI) analysis of the truncated genes/TADs and known and candidate MBS genes from the literature (Table S1) by using the STRING online database (Szklarczyk et al., 2017; https://string-db.org/) with a minimum required interaction score of 0.400.

By mate-pair sequencing, we identified 41 breakpoints in total (Figure S1a and Table S4). As seen on the circos plot (Figure S1c), the breakpoints are clustered within relatively small genomic regions, involving only single chromosomal arms (7q, 8q, and 11p), typical of chromothripsis. No major imbalances were detected using the depth of coverage of the mate-pair reads. Intrachromosomal and interchromosomal structural variants were indicated by 41 BPJs, including 15 translocations, 11 inversions, 7 duplication-type, and 8 deletion-type of rearrangements (Figure S1a,c and Table S5), which have been reported to the Database of Genomic Structural Variation (dbVAR, accession number: nstd161; https://www.ncbi.nlm.nih.gov/dbvar/studies/nstd161/). On the basis of our next-generation sequencing data, we paired the chromosomal fragments together by order and orientation to establish the derivative chromosomes (Figure S1b). At the mate-pair sequencing level the size of the identified fragments varied from ~2.9 kb to ~23.3 Mb. We confirmed 39 of the 41 BPJs (95.1%) by PCR and Sanger sequencing, which also revealed an additional small DNA fragment (135 bp in size) that was deleted between the breakpoints 7-8/7-9 (chr7:92912944–92913075) and inserted into BPJ 7-4_7-11. The sequences of the 39 BPJs at nucleotide resolution revealed the following features: microhomology (2–7 bp) at 20 BPJs; short-templated (8–68 bp) and nontemplated (1–26 bp) insertions at eight BPJs and inserted truncated repeat elements (46 bp from a simple AT-reach repeat and 22 bp from a L1M2 repeat) at two BPJs (Supporting Information S1; Table S5). Furthermore, we observed short deletions (1–877 bp) at 12 breakpoints, short duplications (1–21 bp) at 18, and blunt ends at six breakpoints (Table S4).

The molecular signatures of the breakpoints and the BPJs support replication-independent NHEJ and/or MMEJ as possible underlying mechanisms involved in the repair process (Table S5), typical of chromothripsis (Nazaryan-Petersen & Tommerup, 2016).

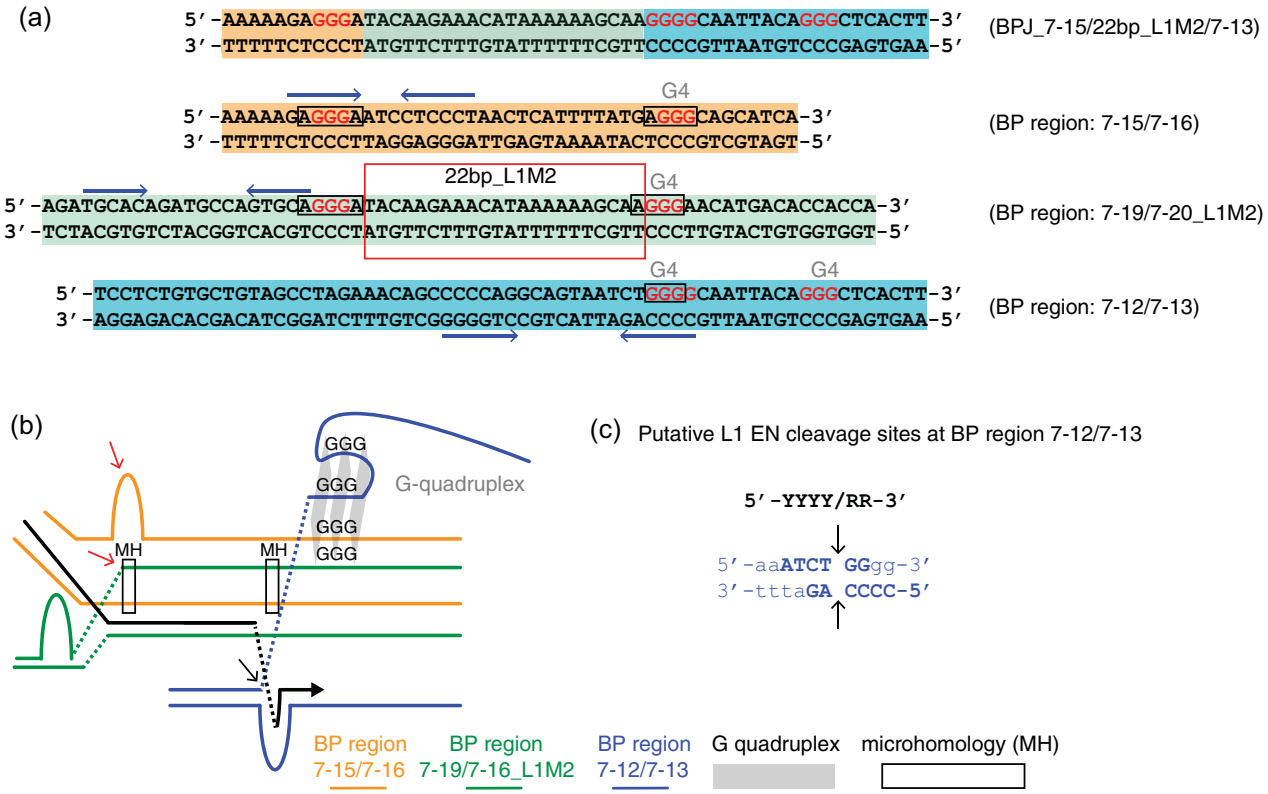

FIGURE 1 Analysis and model for BPJ_7-15/7-13. (a) Sequences from BPJ of derived fragment (top) and donating fragments are shown. Donating fragments are highlighted: fragment 7-15 (orange), 22nt L1M2 insertion (green), and fragment 7-13 (turquoise). Sequence motifs with propensity to form secondary structures are labeled: "G" stretches (red text), "G" stretches proposed to be involved in G-quadruplex formation (G4, gray), and inverted repeats (blue arrows, above or below strand hypothesized to form hairpin). Microhomology at BP-junctions potentially involved in fragment matching and breakpoint resolution between adjacent fragments denoted by block boxes. The 22 bp inserted sequence at the BP-region 7-19/7-20 indicated by red box. (b) Model for chromothriptic intermediate at BPJ 7-15/7-13 before the BPJ resolution. We hypothesize that hairpins formed due to inverted repeats on specific strands spanning BP regions generating fragile sites susceptible to DNA breakage. Donating fragments were stabilized, in part, due to microhomology and the formation of a G-quadruplex (gray parallelograms) involving all three fragments. Known BPs within predicted hairpin structures (red arrows). Small black arrow indicates sequence resembling L1 endonuclease consensus sequence. Dotted line (…) serves to space fragments and facilitate presentation clarity. (c) Sequence at the BP 7-12/7-13 resembles known L1 retrotransposon endonuclease consensus cleavage site. Directionality indicated by 5′ or 3′. Not drawn to scale. BPJ: breakpoint junction; bp: base pair; G: guanine; nt: nucleotide; R: purine; Y: pyrimidine

Notably, we identified 22 bp insertion annotated as L1M2 sequence into BPJ 7-15_7-13 (Figure 1). As we have previously reported that the L1 retrotransposon endonuclease (L1-EN) might mediate *trans* insertions of other repeats at the BPJs in chromothripsis due to the presence of potential L1-EN cleavage sites at the breakpoints (Nazaryan-Petersen et al., 2016), we investigated whether this represented a similar scenario. Several short motifs were present and shared across all three donor fragments (7-15, 7-13, locus for the L1M2 sequence; Figure 1a), including a set of inverted repeats spanning either the 5′- (7-15, L1M2 seq.) or 3′- (7-13) of the donor breakpoint junction. Secondly, stretches of three guanines immediately adjacent to the BP-region 7-15/7-16, L1M2 (BP-region 7-19/7-20), and BP-region 7-12/7-13 were identified. A three guanine nucleotide stretch was identified almost equally spaced between the breaks between the ends of 7-15 and L1M2, which were not joined, within a stretch of microhomology (5′-AGGG-3′). Lastly, a sequence motif resembling the L1 retrotransposon endonuclease consensus cleavage site (5′-YYYY/RR-3, Y-pyrimidine, R-purine) is present on the top-strand of the BP-region 7-12/7-13 and a potentially weaker L1 cut site on the bottom strand (Hancks & Kazazian, 2016). We postulate that the donor fragments were positioned and maintained in place potentially due to microhomologies involving G–C basepairing (Figure 1c). Subsequently, a cascade triggered by hairpin formation of IRs on specific strands resulted in fragile sites susceptible to DNA-damaging agents, which may have included L1 ORF2 EN, and breathing strands—that formed a G-quadruplex to stabilize and promote the derived configuration.

The breakpoints truncated 12 protein-coding genes and three highly conserved TADs (Dixon et al., 2012) as candidate regulatory domains for developmental (evo–devo) genes (Table S2 and Figure S1c). At four BPJs, the truncated genes were joined together in the same orientation (Table S5), however no potential fusion protein is predicted (Supporting Information S2). In silico PPI analysis of the truncated genes/TADs involved in the CCR (Table S1) and the published known and candidate MBS genes (Table S2) revealed four truncated genes, including *SEMA3A* (sema domain, immunoglobulin domain [Ig], short basic domain,

secreted, semaphorin 3A; MIM# 603961), *SEMA3D* (sema domain, immunoglobulin domain [Ig], short basic domain, secreted, semaphorin 3D; MIM# 609907), *PIK3CG* (phosphatidylinositol-4,5-bisphosphate 3-kinase, catalytic subunit γ; MIM# 601232), and *UBR5* (ubiquitin protein ligase E3 component n-recognin 5; MIM# 608413), as well as one TAD harboring *FZD1* (frizzled family receptor 1; MIM# 603408), that form an interactive cluster with the two known MBS-associated genes *PLXND1* and *REV3L*; *TUBB3*; and six suggested candidate genes (*PLXNA1*, MIM# 601055; *FLT1*, MIM# 165070; *FGF9*, MIM# 600921; *KIF21A*, MIM# 608283; *GATA2*, MIM# 137295; and *SOX14*, MIM# 604747), based on experiments, coexpression, curated databases, and "text-mining" (Figure 2). On the basis of this interactive cluster, we performed literature review to better understand the functional link between known and candidate MBS genes and the genes truncated by the present CCR.

Though functional interactions between the different classes of plexins and semaphorins are well established, and although *PLXNA1* and *PLXND1* have been suggested to be attractive candidate genes for MBS for many years (Kremer et al., 1996), and mutations in *PLXND1* in MBS patients have been reported recently (Tomas-Roca et al., 2015), semaphorins have not been considered as candidates for MBS to date. Plexins and neuropilins are the primary semaphorin receptors, which through signal transduction play important roles in repulsive axon guidance to direct neuronal axons to their appropriate targets (Takamatsu & Kumanogoh, 2012). Consistently, Sema3A is required for the development of the facial nerve in the mouse (Schwarz et al., 2008). In addition, studies of chick and mouse embryos have demonstrated that Sema3a is highly expressed in endothelial cells of blood vessels and that *Sema3a*-null mice show vascular defects, suggesting that Sema3a is involved in angiogenesis (Serini et al., 2003). Notably, abnormal vascular supply during embryogenesis has been proposed as a possible cause for MBS (D'Cruz et al., 1993; Kadakia et al., 2015). Moreover, heterozygous mutations in *SEMA3A* have been associated with Kallmann syndrome (hypogonadotropic hypogonadism 16 with or without anosmia; MIM# 614897; Hanchate et al., 2012), which may occasionally coappear with MBS (Lopez de Lara, Cruz-Rojo, Sanchez del Pozo, Gallego Gomez, & Lledo Valera, 2008; Rubinstein, Lovelace, Behrens, & Weisberg, 1975). However, as in some patients *SEMA3A* mutations coincided with mutations in other known Kallmann syndrome genes, Hanchate et al. (2012) suggested that the monoallelic mutations in *SEMA3A* contribute to the pathogenesis of Kallmann syndrome rather than initiate the disease. To our knowledge, the patient studied here did not have hypogonadism or olfactory defects, indicating that other genes involved in Kallmann syndrome might be intact. Thus, we posit that truncation of *SEMA3A* in our patient is the most likely reason for the MBS features, and that *SEMA3A* screening of MBS patients (especially those associated with Kallmann syndrome) is highly warranted. In addition, truncation of *SEMA3D* might also have an additive effect in developing MBS in our patient, as Sema3D is reported to play a role in inducing the collapse and paralysis of neuronal growth cones which could potentially act as repulsive cues toward specific neuronal populations, as demonstrated in zebrafish (Liu & Halloran, 2005). Moreover, as *SEMA3E* is located ~300 kb proximal to *SEMA3A* within a large TAD in IMR90 cells that harbor *SEMA3A*, *SEMA3D*, and *SEMA3E* (Rao et al., 2014; http://promoter.bx.psu.edu/hi-c/index.html; Figure S2), we suggest that long-range dysregulation of *SEMA3E* could also impact on MBS phenotype, We further noticed that two of the truncated genes, *SEMA3A* and *PIK3CG*, encode proteins that are functionally linked together via FLT1 (Figure 2), which has been proposed as a candidate MBS locus (Slee, Smart, & Viljoen, 1991). *FLT1* encodes a tyrosine-protein kinase that acts as a cell-surface receptor for VEGF (vascular

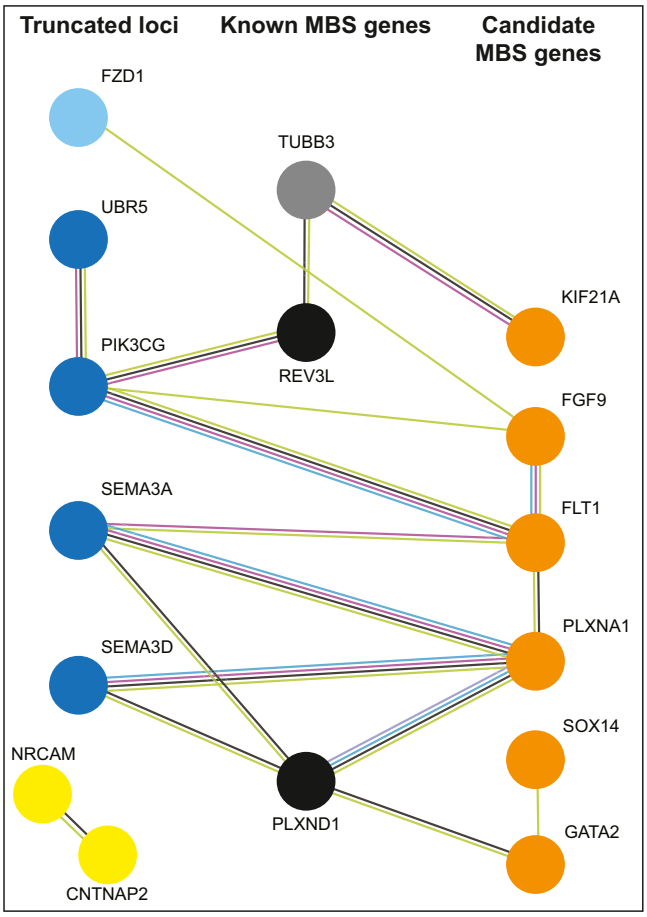

FIGURE 2 In silico protein–protein interaction between truncated genes/TADs by the chromothripsis breakpoints and known/candidate genes involved in Moebius syndrome. STRING online database (Szklarczyk et al., 2017) was used to analyze the association between the truncated genes (blue), potential regulatory domains (light blue; Table S2), published known (black, grey) and candidate MBS genes (orange; Table S1). Candidate intellectual disability (ID) genes are yellow. Each node represents all the alternative transcript variants produced by single protein-coding gene locus. Edges represent protein–protein associations, which might indicate that the proteins contribute to a shared function but not necessarily physically bind each other. Blue interactions are based on curated databases; pink interactions are proved experimentally; yellow interactions indicate that the proteins are comentioned in PubMed abstracts; and black interactions indicate that the proteins are coexpressed. MBS: Moebius syndrome; TAD: topological associated domain

endothelial growth factor), and plays an essential role in the development of embryonic vasculature and angiogenesis. Also, VEGF is activated upon binding with Flt1 receptors inducing the migration of brain microvascular endothelial cells in the rat via a pathway, where PI3K is involved (Radisavljevic, Avraham, & Avraham, 2000). Semaphorin 3A may attract tumor associated macrophages via plexinA1/plexinA4 and neuropilin-1 holoreceptor followed by Flt1 activation, leading to immunosuppression and angiogenesis in mouse tumor models (Casazza et al., 2013). Furthermore, the truncated *UBR5* encodes an evolutionary conserved interactor of PI3K (Breitkopf et al., 2016) which has been implicated in various aspects of vessel formation. Finally, the in silico PPI indicates an association between PIK3CG and REV3L (Hirano & Sugimoto, 2006), which has been established to play a role in MBS (Tomas-Roca et al., 2015).

While intellectual disability has been described in association with MBS, a clinical study of a Dutch MBS cohort reported that most likely this is not true, as MBS patients are unable to express their emotions via facial expression and may have severe lack of speech, giving a false impression of intellectual disability (Verzijl, van Es, Berger, Padberg, & van Spaendonck, 2005). Therefore, we hypothesize that the presence of intellectual disability in our patient is likely a result of another truncated gene(s) playing a role in brain development, for example, *NRCAM* (neuronal cell adhesion molecule, MIM# 601581; Demyanenko et al., 2014) and *CNTNAP2* (contactin associated protein-like 2; MIM# 604569; Smogavec et al., 2016).

In conclusion, de novo mutations in *PLXND1* and *REV3L* have been found in only a small fraction of MBS patients (Tomas-Roca et al., 2015) indicating that additional genes might play a role. Several genes (*SEMA3A*, *SEMA3D*, *PIK3CG*, and *UBR5*) truncated by the present chromothripsis breakpoints may actually link together *PLXND1* and *REV3L* (Figure 2), which were considered to represent independent pathways involved in hindbrain development (Tomas-Roca et al., 2015). Our findings suggest that the simultaneous truncation of several interactors of the known MBS genes by the multiple breakpoints of a germline chromothripsis may result in a complex multigenic disorder. Whether this is facilitated by a propensity for functional related loci to be in closer proximity when the damage occurred, for example, via "chromosome kissing" (Cavalli, 2007), or it reflects the selection we make by focusing on a specific phenotype, is unknown. Specifically, our study implies that the screening for single or additive variants within the semaphorin–plexin pathway should be attempted in the MBS cohorts. At a general level, it suggests that the truncated loci in other cases of CCRs should be analysed in the context of functional interactions.

ACKNOWLEDGMENTS

This study was supported by the Danish Council for Independent Research (4183-00482B), the University of Copenhagen Excellence Programme for Interdisciplinary Research (Global Genes, Local Concerns), and the Lundbeck Foundation (Genetics in Cognitive Comorbidity II-[2013–14290]). D.C.H. is funded by a NIH K99/R00 Pathway to Independence Award (NIGMS) and a Cancer Prevention Research Institute of Texas (CPRIT) Recruitment Award. We thank the family for participating in the study.

CONFLICT OF INTERESTS

The authors declare that there are no conflict of interests.

ORCID

Lusine Nazaryan-Petersen http://orcid.org/0000-0002-4807-6827
Vera M. Kalscheuer http://orcid.org/0000-0001-6898-3259

REFERENCES

Borck, G., Wirth, J., Hardt, T., Tonnies, H., Brondum-Nielsen, K., Bugge, M., … Haaf, T. (2001). Molecular cytogenetic characterisation of a complex 46,XY,t(7;8;11;13) chromosome rearrangement in a patient with Moebius syndrome. *Journal of Medical Genetics*, *38*(2), 117–121.

Breitkopf, S. B., Yang, X., Begley, M. J., Kulkarni, M., Chiu, Y.-H., Turke, A. B., … Asara, J. M. (2016). A cross-species study of PI3K protein-protein interactions reveals the direct interaction of P85 and SHP2. *Scientific Reports*, *6*, 20471. https://doi.org/10.1038/srep20471

Broussard, A. B., & Borazjani, J. G. (2008). The faces of Moebius syndrome: Recognition and anticipatory guidance. *MCN. The American Journal of Maternal Child Nursing*, *33*(5), 272–280. https://doi.org/10.1097/01.NMC.0000334892.45979.d5

Casazza, A., Laoui, D., Wenes, M., Rizzolio, S., Bassani, N., Mambretti, M., … Mazzone, M. (2013). Impeding macrophage entry into hypoxic tumor areas by Sema3A/Nrp1 signaling blockade inhibits angiogenesis and restores antitumor immunity. *Cancer Cell*, *24*(6), 695–709. https://doi.org/10.1016/j.ccr.2013.11.007

Cavalli, G. (2007). Chromosome kissing. *Current Opinion in Genetics & Development*, *17*(5), 443–450. https://doi.org/10.1016/j.gde.2007.08.013

D'Cruz, O. F., Swisher, C. N., Jaradeh, S., Tang, T., & Konkol, R. J. (1993). Mobius syndrome: Evidence for a vascular etiology. *Journal of Child Neurology*, *8*(3), 260–265. https://doi.org/10.1177/088307389300800310

Demyanenko, G. P., Mohan, V., Zhang, X., Brennaman, L. H., Dharbal, K. E. S., Tran, T. S., … Maness, P. F. (2014). Neural cell adhesion molecule NrCAM regulates Semaphorin 3F-induced dendritic spine remodeling. *The Journal of Neuroscience*, *34*(34), 11274–11287. https://doi.org/10.1523/JNEUROSCI.1774-14.2014

Dixon, J. R., Selvaraj, S., Yue, F., Kim, A., Li, Y., Shen, Y., … Ren, B. (2012). Topological domains in mammalian genomes identified by analysis of chromatin interactions. *Nature*, *485*(7398), 376–380. https://doi.org/10.1038/nature11082

Donahue, S. P., Wenger, S. L., Steele, M. W., & Gorin, M. B. (1993). Broad-spectrum Mobius syndrome associated with a 1;11 chromosome translocation. *Ophthalmic Paediatrics and Genetics*, *14*(1), 17–21.

Hanchate, N. K., Giacobini, P., Lhuillier, P., Parkash, J., Espy, C., Fouveaut, C., … Dode, C. (2012). SEMA3A, a gene involved in axonal pathfinding, is mutated in patients with Kallmann syndrome. *PLOS Genetics*, *8*(8), e1002896. https://doi.org/10.1371/journal.pgen.1002896

Hancks, D. C., & Kazazian, H. H. J. (2016). Roles for retrotransposon insertions in human disease. *Mobile DNA*, *7*, 9. https://doi.org/10.1186/s13100-016-0065-9

Hirano, Y., & Sugimoto, K. (2006). ATR homolog Mec1 controls association of DNA polymerase zeta-Rev1 complex with regions near a double-strand break. *Current Biology*, *16*(6), 586–590. https://doi.org/10.1016/j.cub.2006.01.063

Kadakia, S., Helman, S. N., Schwedhelm, T., Saman, M., & Azizzadeh, B. (2015). Examining the genetics of congenital facial paralysis—a closer look at Moebius syndrome. *Oral and Maxillofacial Surgery*, *19*(2), 109–116. https://doi.org/10.1007/s10006-015-0485-6

Kremer, H., Kuyt, L. P., van den Helm, B., van Reen, M., Leunissen, J. A., Hamel, B. C., … Padberg, G. W. (1996). Localization of a gene for Mobius syndrome to chromosome 3q by linkage analysis in a Dutch family. *Human Molecular Genetics*, *5*(9), 1367–1371.

Lieber, M. R. (2010). The mechanism of double-strand DNA break repair by the nonhomologous DNA end-joining pathway. *Annual Review of Biochemistry*, *79*, 181–211. https://doi.org/10.1146/annurev.biochem.052308.093131

Liu, Y., & Halloran, M. C. (2005). Central and peripheral axon branches from one neuron are guided differentially by Semaphorin 3D and transient axonal glycoprotein-1. *The Journal of Neuroscience*, *25*(45), 10556–10563. https://doi.org/10.1523/JNEUROSCI.2710-05.2005

Lopez de Lara, D., Cruz-Rojo, J., Sanchez del Pozo, J., Gallego Gomez, M. E., & Lledo Valera, G. (2008). Moebius-Poland syndrome and hypogonadotropic hypogonadism. *European Journal of Pediatrics*, *167*(3), 353–354. https://doi.org/10.1007/s00431-007-0473-4

McVey, M., & Lee, S. E. (2008). MMEJ repair of double-strand breaks (director's cut): Deleted sequences and alternative endings. *Trends in Genetics: TIG*, *24*(11), 529–538. https://doi.org/10.1016/j.tig.2008.08.007

Nakamura, Y., Matsumoto, H., Zaha, K., Uematsu, K., & Nonoyama, S. (2018). TUBB3 E410K syndrome with osteoporosis and cough syncope in a patient previously diagnosed with atypical Moebius syndrome. *Brain & Development*, *40*(3), 233–237. https://doi.org/10.1016/j.braindev.2017.12.006

Nazaryan, L., Stefanou, E. G., Hansen, C., Kosyakova, N., Bak, M., Sharkey, F. H., … Tommerup, N. (2014). The strength of combined cytogenetic and mate-pair sequencing techniques illustrated by a germline chromothripsis rearrangement involving FOXP2. *European Journal of Human Genetics*, *22*(3), 338–343. https://doi.org/10.1038/ejhg.2013.147

Nazaryan-Petersen, L., Bertelsen, B., Bak, M., Jonson, L., Tommerup, N., Hancks, D. C., & Tumer, Z. (2016). Germline chromothripsis driven by L1-mediated retrotransposition and Alu/Alu homologous recombination. *Human Mutation*, *37*(4), 385–395. https://doi.org/10.1002/humu.22953

Nazaryan-Petersen, L., & Tommerup, N. (2016). Chromothripsis and human genetic disease, *eLS*. Chichester, UK: John Wiley & Sons, Ltd. https://doi.org/ 10.1002/9780470015902.a0024627.

Patel, R. M., Liu, D., Gonzaga-Jauregui, C., Jhangiani, S., Lu, J. T., Sutton, V. R., … Campeau, P. M. (2017). An exome sequencing study of Moebius syndrome including atypical cases reveals an individual with CFEOM3A and a TUBB3 mutation. *Cold Spring Harbor Molecular Case Studies*, *3*, 000984. https://doi.org/10.1101/mcs.a000984

Radisavljevic, Z., Avraham, H., & Avraham, S. (2000). Vascular endothelial growth factor up-regulates ICAM-1 expression via the phosphatidylinositol 3 OH-kinase/AKT/Nitric oxide pathway and modulates migration of brain microvascular endothelial cells. *The Journal of Biological Chemistry*, *275*(27), 20770–20774. https://doi.org/10.1074/jbc.M002448200

Rao, S. S. P., Huntley, M. H., Durand, N. C., Stamenova, E. K., Bochkov, I. D., Robinson, J. T., … Aiden, E. L. (2014). A 3D map of the human genome at kilobase resolution reveals principles of chromatin looping. *Cell*, *159*(7), 1665–1680. https://doi.org/10.1016/j.cell.2014.11.021

Rubinstein, A. E., Lovelace, R. E., Behrens, M. M., & Weisberg, L. A. (1975). Moebius syndrome in Kallmann syndrome. *Archives of Neurology*, *32*(7), 480–482.

Schwarz, Q., Waimey, K. E., Golding, M., Takamatsu, H., Kumanogoh, A., Fujisawa, H., … Ruhrberg, C. (2008). Plexin A3 and plexin A4 convey semaphorin signals during facial nerve development. *Developmental Biology*, *324*(1), 1–9. https://doi.org/10.1016/j.ydbio.2008.08.020

Serini, G., Valdembri, D., Zanivan, S., Morterra, G., Burkhardt, C., Caccavari, F., … Bussolino, F. (2003). Class 3 semaphorins control vascular morphogenesis by inhibiting integrin function. *Nature*, *424*(6947), 391–397. https://doi.org/10.1038/nature01784

Slee, J. J., Smart, R. D., & Viljoen, D. L. (1991). Deletion of chromosome 13 in Moebius syndrome. *Journal of Medical Genetics*, *28*(6), 413–414.

Smogavec, M., Cleall, A., Hoyer, J., Lederer, D., Nassogne, M.-C., Palmer, E. E., … Zweier, C. (2016). Eight further individuals with intellectual disability and epilepsy carrying bi-allelic CNTNAP2 aberrations allow delineation of the mutational and phenotypic spectrum. *Journal of Medical Genetics*, *53*(12), 820–827. https://doi.org/10.1136/jmedgenet-2016-103880

Szklarczyk, D., Morris, J. H., Cook, H., Kuhn, M., Wyder, S., Simonovic, M., … von Mering, C. (2017). The STRING database in 2017: Quality-controlled protein-protein association networks, made broadly accessible. *Nucleic Acids Research*, *45*(D1), D362–D368. https://doi.org/10.1093/nar/gkw937

Takamatsu, H., & Kumanogoh, A. (2012). Diverse roles for semaphorin-plexin signaling in the immune system. *Trends in Immunology*, *33*(3), 127–135. https://doi.org/10.1016/j.it.2012.01.008

Tomas-Roca, L., Tsaalbi-Shtylik, A., Jansen, J. G., Singh, M. K., Epstein, J. A., Altunoglu, U., … van Bokhoven, H. (2015). De novo mutations in PLXND1 and REV3L cause Mobius syndrome. *Nature Communications*, *6*, 7199. https://doi.org/10.1038/ncomms8199

Uzumcu, A., Karaman, B., Toksoy, G., Uyguner, Z. O., Candan, S., Eris, H., … Basaran, S. (2009). Molecular genetic screening of MBS1 locus on chromosome 13 for microdeletions and exclusion of FGF9, GSH1 and CDX2 as causative genes in patients with Moebius syndrome. *European Journal of Medical Genetics*, *52*(5), 315–320. https://doi.org/10.1016/j.ejmg.2009.05.003

Verzijl, H. T. F. M., van Es, N., Berger, H. J. C., Padberg, G. W., & van Spaendonck, K. P. M. (2005). Cognitive evaluation in adult patients with Mobius syndrome. *Journal of Neurology*, *252*(2), 202–207. https://doi.org/10.1007/s00415-005-0637-y

Verzijl, H. T. F. M., van der Zwaag, B., Cruysberg, J. R. M., & Padberg, G. W. (2003). Mobius syndrome redefined: A syndrome of rhombencephalic maldevelopment. *Neurology*, *61*(3), 327–333.

Ziter, F. A., Wiser, W. C., & Robinson, A. (1977). Three-generation pedigree of a Mobius syndrome variant with chromosome translocation. *Archives of Neurology*, *34*(7), 437–442.

van der Zwaag, B., Verzijl, H., d Beltran-Valero, Schuster, V., van Bokhoven, H., Kremer, H., … Padberg, G. (2002). Mutation analysis in the candidate Möbius syndrome genes PGT and GATA2 on chromosome 3 and EGR2 on chromosome 10. *Journal of Medical Genetics*, *39*, e30–e30. https://doi.org/10.1136/jmg.39.6.e30

van der Zwaag, B., Verzijl, H. T., Wichers, K. H., Beltran-Valero de Bernabe, D., Brunner, H. G., van Bokhoven, H., & Padberg, G. W. (2004). Sequence analysis of the PLEXIN-D1 gene in Mobius syndrome patients. *Pediatric Neurology*, *31*(2), 114–118. https://doi.org/10.1016/j.pediatrneurol.2004.02.004

SUPPORTING INFORMATION

Additional supporting information may be found online in the Supporting Information section at the end of the article.

How to cite this article: Nazaryan-Petersen L, Oliveira IR, Mehrjouy MM, et al. Multigenic truncation of the semaphorin–plexin pathway by a germline chromothriptic rearrangement associated with Moebius syndrome. *Human Mutation*. 2019;40:1057–1062. https://doi.org/10.1002/humu.23775